

The Role of Linear Layers in Nonlinear Interpolating Networks

Greg Ongie* & Rebecca Willett†

February 3, 2022

Abstract

This paper explores the implicit bias of overparameterized neural networks of depth greater than two layers. Our framework considers a family of networks of varying depth that all have the same *capacity* but different implicitly defined *representation costs*. The representation cost of a function induced by a neural network architecture is the minimum sum of squared weights needed for the network to represent the function; it reflects the function space bias associated with the architecture. Our results show that adding linear layers to a ReLU network yields a representation cost that reflects a complex interplay between the alignment and sparsity of ReLU units. Specifically, using a neural network to fit training data with minimum representation cost yields an interpolating function that is constant in directions perpendicular to a low-dimensional subspace on which a parsimonious interpolant exists.

1 Introduction

An outstanding problem in understanding the generalization properties of overparameterized neural networks is to characterize which functions are best represented by neural networks of varying architectures. Past work explored the notion of *representation costs* – i.e., how much does it “cost” for a neural network to represent some function f . Specifically, the representation cost of a function f is the minimum sum of squared network weights necessary for the network to represent f .

The following key question then arises: **How does network depth affect which functions have minimum representation cost?** For instance, given a set of training samples, say we find the interpolating function that minimizes the representation cost; how is that interpolant different for a network with three layers instead of two layers? Both functions have the same values on the training samples, but they may have very different behaviors elsewhere in the domain.

In this paper, we describe the representation cost of a family of networks with L layers in which $L - 1$ layers have linear activations and the final layer has a ReLU activation. As detailed in §1.1, networks related to this class play an important role in both theoretical studies of neural network generalization properties and experimental efforts. One reason that this is a particularly important family to study is that adding linear layers does not change the capacity or expressivity of a network, even though the number of parameters may change; this means that different behaviors for different depths solely reflects the role of depth and not of capacity.

We show that adding linear layers to a ReLU network with weight decay regularization is akin to using a two-layer ReLU network with nuclear or Schatten norm regularization on the weight matrix. This insight suggests that lower-rank weight matrices, corresponding to aligned ReLU units, will be favored. However, the representation costs we derive provide a nuanced perspective that extends beyond “linear layers promote alignment”, as illustrated in Figure 1 and Figure 2. In particular, the effect of linear layers, as understood through the corresponding representation costs, reflects a subtle interplay between ReLU unit alignment

*G. Ongie is with the Department of Mathematical and Statistical Sciences, Marquette University, Milwaukee, WI, USA. e-mail: gregory.ongie@marquette.edu

†R. Willett is with the Department of Statistics and Department of Computer Science, University of Chicago, Chicago, IL, USA.

and the magnitudes of the outer layer weights. We find that lower representation costs are associated with functions that can be parsimoniously expressed using only the orthogonal projection of their inputs onto a low-dimensional subspace.

1.1 Related work

Past work has explored the role of neural network depth via a “depth separation” analysis (e.g. Daniely (2017); Vardi and Shamir (2020)); these analyses identify functions which may be efficiently represented at one depth but require an exponential width to represent them with fewer layers. This line of work has yielded important insights into the role of depth, but recent work has highlighted how functions leading to depth separation results are often highly oscillatory and perhaps not fully capturing the import of depth in practical settings (i.e., may be “worse case” but not “average case” results). In particular, Safran et al. (2019) shows that if the Lipschitz constant of the target function is kept fixed, then existing depth separation results between 2- and 3-layer nets do not hold.

A number of papers have studied representation costs and implicit regularization from a function space perspective associated with neural networks. Following a univariate analysis by Savarese et al. (2019), Ongie et al. (2019) considers two-layer multivariate ReLU networks where the hidden layer has infinite width:

$$\lim_{K \rightarrow \infty} \sum_{k=1}^K a_k [\mathbf{w}_k^\top \mathbf{x} + b_k]_+.$$

Recent work by Mulayoff et al. (2021) connects the function space representation costs of two-layer ReLU networks to the stability of SGD minimizers.

Gunasekar et al. (2018) shows that L -layer *linear* networks with *diagonal* structure induces a non-convex implicit bias over network weights corresponding to the ℓ^q norm of the outer layer weights for $q = 2/L$; similar conclusions hold for deep *linear* convolutional networks. Recent work by Dai et al. (2021) examines the representation costs of deep *linear* networks from a function space perspective. However, the existing literature does not fully characterize the representation costs of *deep, non-linear* networks from a function space perspective. Parhi and Nowak (2021) consider deeper networks and define a compositional function space with a corresponding representer theorem; the properties of this function space and the role of depth are an area of active investigation.

Our paper focuses on the role of linear layers in *nonlinear* networks. The role of linear layers in such settings has been explored in a number of works. Golubeva et al. (2020) looks at the role of network *width* when the number of parameters is held fixed; it specifically looks at increasing the width without increasing the number of parameters by adding linear layers. This procedure seems to help with generalization performance (as long as the training error is controlled). However, Golubeva et al. (2020) note that the implicit regularization caused by this approach is not understood. *One of the main contributions of our paper is a better understanding of this implicit regularization.*

The effect of linear layers on training speed was previously examined by Ba and Caruana (2013); Urban et al. (2016). Arora et al. (2018) considers implicit acceleration in deep nets and claims that depth induce a momentum-like term in training deep *linear* networks with SGD, though the regularization effects of this acceleration are not well understood. Implicit regularization of gradient descent has been studied in the context of matrix and tensor factorization problems Gunasekar et al. (2018); Arora et al. (2019); Razin and Cohen (2020); Razin et al. (2021). Similar to this work, low-rank representations play a key role in their analysis.

1.2 Notation

For a vector $\mathbf{a} \in \mathbb{R}^K$, we use $\|\mathbf{a}\|_p$ to denote its ℓ^p norm. For a matrix \mathbf{W} , we use $\|\mathbf{W}\|_F$ to denote the Frobenius norm, $\|\mathbf{W}\|_*$ to denote its nuclear norm (i.e., the sum of the singular values), and for $0 < q \leq 1$ we use $\|\mathbf{W}\|_{S_q}$ to denote its Schatten- q quasi-norm (i.e., the ℓ^q quasi-norm of the singular values of a matrix \mathbf{W}). Given a vector $\mathbf{a} \in \mathbb{R}^K$, the matrix $\mathbf{D}_\mathbf{a} \in \mathbb{R}^{K \times K}$ is a diagonal matrix with the entries of \mathbf{a} along the diagonal.

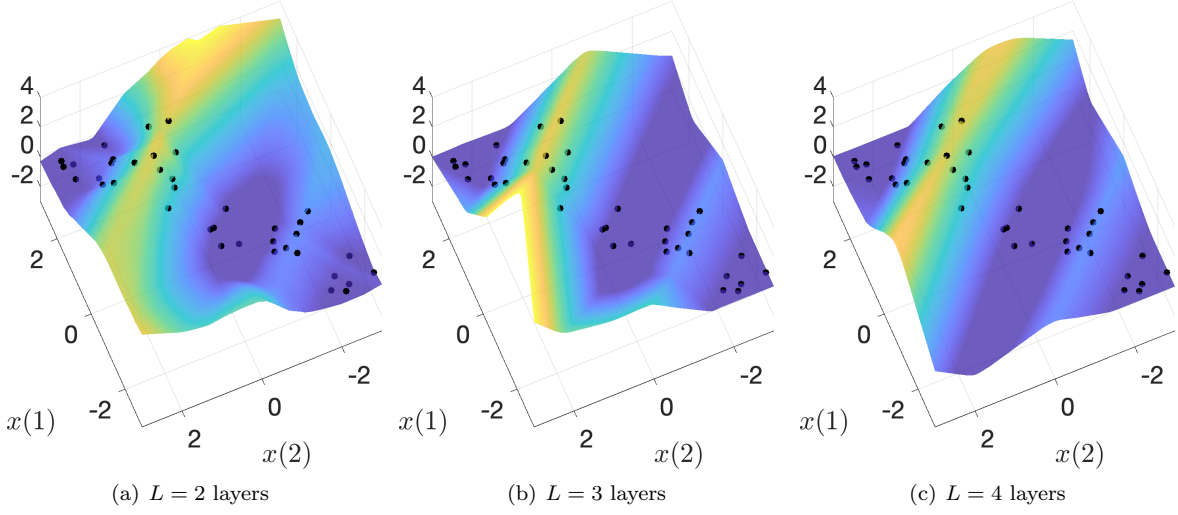


Figure 1: **Numerical evidence that weight decay promotes unit alignment with more linear layers.** Neural networks with $L - 1$ linear layers plus one ReLU layer were trained using SGD with weight decay regularization to close to zero training loss on the training samples, as shown in black. Pictured in (a)-(c) are the resulting interpolating functions shown as surface plots. Our theory predicts that as the number of linear layers increases, the learned interpolating function will become closer to constant in directions perpendicular to a low-dimensional subspace on which a parsimonious interpolant can be defined.

For a vector $\mathbf{\lambda}$, we write $\mathbf{\lambda} > 0$ to indicate it has all positive entries. Finally, we use $[t]_+ = \max\{0, t\}$ to denote the ReLU activation, and whose application to vectors is understood entrywise.

2 Definitions

Let $N_2(\mathbb{R}^d)$ denote the space of functions expressible as a two-layer ReLU network having input dimension d and such that the width K of the single hidden layer is unbounded. Every function in $N_2(\mathbb{R}^d)$ is described (non-uniquely) by a collection of weights $\theta = (\mathbf{W}, \mathbf{a}, \mathbf{b}, c)$:

$$h_{\theta}^{(2)}(\mathbf{x}) = \mathbf{a}^\top [\mathbf{W}\mathbf{x} + \mathbf{b}]_+ + c. \quad (1)$$

$$= \sum_{k=1}^K a_k [\mathbf{w}_k^\top \mathbf{x} + b_k]_+ + c \quad (2)$$

with $\mathbf{W} \in \mathbb{R}^{K \times d}$, $\mathbf{a}, \mathbf{b} \in \mathbb{R}^K$ and $c \in \mathbb{R}$. We denote the set of all such parameter vectors θ by Θ_2 .

In this work, we consider a re-parameterization of networks in $N_2(\mathbb{R}^d)$. Specifically, we replace the linear input layer \mathbf{W} with $L - 1$ linear layers:

$$h_{\theta}^{(L)}(\mathbf{x}) = \mathbf{a}^\top [\mathbf{W}_{L-1} \cdots \mathbf{W}_2 \mathbf{W}_1 \mathbf{x} + \mathbf{b}]_+ + c \quad (3)$$

where now $\theta = (\mathbf{W}_1, \mathbf{W}_2, \dots, \mathbf{W}_{L-1}, \mathbf{a}, \mathbf{b}, c)$. Again, we allow the widths of all layers to be arbitrarily large. Let Θ_L denote the set of all such parameter vectors. With any $\theta \in \Theta_L$ we associate the cost

$$C_L(\theta) = \frac{1}{L} (\|\mathbf{a}\|_2^2 + \|\mathbf{W}_1\|_F^2 + \cdots + \|\mathbf{W}_{L-1}\|_F^2), \quad (4)$$

i.e., the squared Euclidean norm of all non-bias weights.

Given training pairs $\{(\mathbf{x}_i, y_i)\}_{i=1}^n$, consider the problem of finding a L -layer network with minimal cost C_L that interpolates the training data:

$$\min_{\theta \in \Theta_L} C_L(\theta) \quad \text{s.t.} \quad h_{\theta}^{(L)}(\mathbf{x}_i) = y_i \quad (5)$$

This optimization is akin to training a network to interpolate training data using SGD with squared ℓ^2 norm or weight decay regularization Hanson and Pratt (1988); Loshchilov and Hutter (2017). We may recast this as an optimization problem in function space: for any $f \in N_2(\mathbb{R}^d)$, define its L -layer representation cost $R_L(f)$ by

$$R_L(f) = \min_{\theta} C_L(\theta) \quad \text{s.t.} \quad f = h_{\theta}^{(L)}. \quad (6)$$

Then (5) is equivalent to:

$$\min_{f \in N_2} R_L(f) \quad \text{s.t.} \quad f(\mathbf{x}_i) = y_i. \quad (7)$$

Earlier work such as Savarese et al. (2019) has shown that

$$R_2(f) = \min_{\theta \in \Theta_2} \|\mathbf{a}\|_1 \quad \text{s.t.} \quad \|\mathbf{w}_k\|_2 = 1, \quad (8)$$

$$\forall k = 1, \dots, K \text{ and } f = h_{\theta}^{(2)}$$

Our goal is to characterize the representation cost R_L for different numbers of layers $L \geq 3$, and describe how the set of global minimizers of (7) changes with L , providing insight into the role of linear layers in nonlinear ReLU networks.

3 Simplifying the Representation Cost

Here we derive simplified expressions for the representation costs R_L with $L \geq 3$. Proofs of all results in this section are given in Appendix A

Our first result shows that if the predictor function is univariate then the R_L representation cost reduces to the $2/L$ -power of the R_2 representation cost:

Theorem 3.1. *If $f \in N_2(\mathbb{R}^1)$ (i.e., f is univariate) then*

$$R_L(f) = [R_2(f)]^{2/L}. \quad (9)$$

This shows that L -layer minimum norm interpolants in 1-D coincide with 2-layer minimum norm interpolants, as characterized by Savarese et al. (2019); Hanin (2019).

However, in the multivariate setting, where the input dimension $d > 1$, the R_L -costs with $L \geq 3$ are not simply a monotonic transform of the R_2 -cost, as we now show.

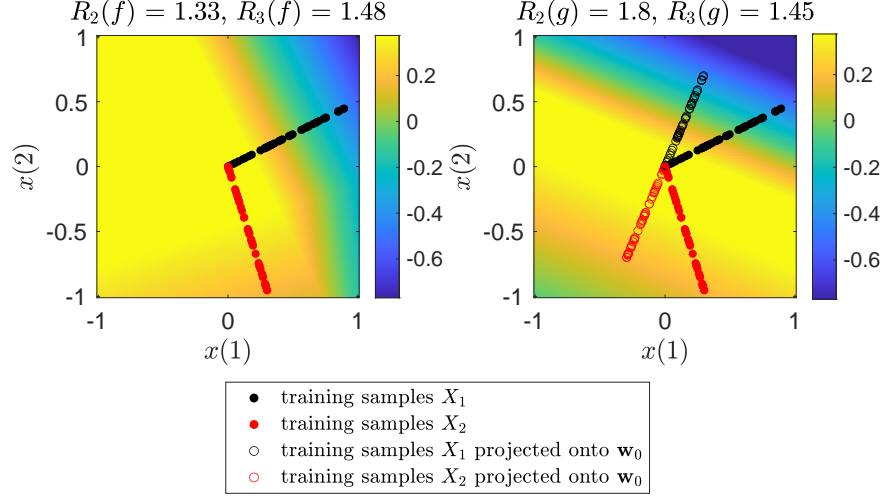
First, we prove that the general R_L -cost can be re-cast as an optimization over two-layer networks, but where the representation cost associated with the inner-layer weight matrix \mathbf{W} changes with L :

Lemma 3.2. *Suppose $f \in N_2(\mathbb{R}^d)$. Then*

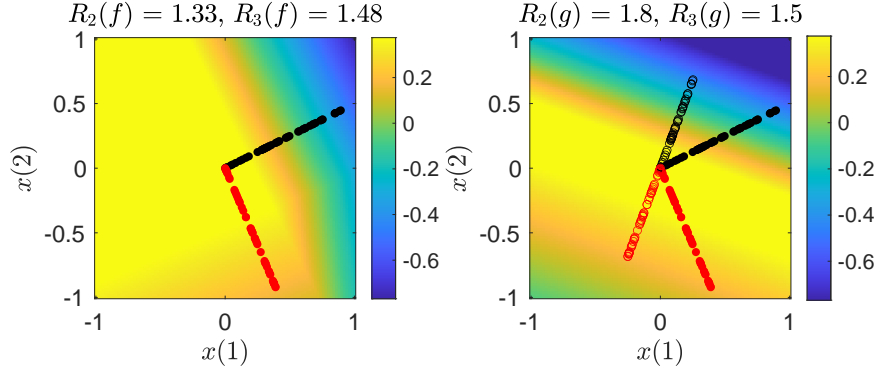
$$R_L(f) = \min_{\theta \in \Theta_2} \frac{1}{L} \|\mathbf{a}\|_2^2 + \frac{L-1}{L} \|\mathbf{W}\|_{\mathcal{S}^q}^q \quad \text{s.t.} \quad f = h_{\theta}^{(2)} \quad (10)$$

where $q := 2/(L-1)$ and $\|\mathbf{W}\|_{\mathcal{S}^q}$ is the Schatten- q quasi-norm, i.e., the ℓ^q quasi-norm of the singular values of \mathbf{W} .

Note that Schatten- q quasi-norms with $0 < q \leq 1$ are often used as a surrogate for the rank penalty. Intuitively, this shows that minimizing the R_L -cost for $L \geq 3$ ought to promote low-rank inner-layer weight matrices \mathbf{W} , and this bias should become more pronounced as L grows. However, the reduced form of the



(a) *Left*: Minimum R_2 interpolant when samples lie on two rays separated by an angle of 0.55π . *Right*: Minimum R_3 interpolant of same data.



(b) *Left*: Minimum R_2 interpolant when samples lie on two rays separated by an angle of 0.52π . *Right*: Interpolant of same data with aligned ReLU units **does not** minimize R_3 .

Figure 2: **Adding linear layers does not always promote alignment of ReLU units.** (a) Samples lie on two rays separated by 0.55π . The minimum R_2 interpolant f is quite different from the minimum R_3 interpolant g , where the latter has ReLU units aligned with a subspace that is the difference between the two rays. (b) Here the rays are only separated by 0.52π , and the minimum R_2 interpolant f also has a smaller R_3 representation cost than the interpolant with aligned ReLU units. This example illustrates that *ReLU alignment alone does not capture representation costs of deeper networks*.

R_2 -cost in (8) suggests that sparsity of the outer-layer weights \mathbf{a} ought to also play a role in determining the R_L -cost for $L > 2$, yet this dependence is not explicitly revealed in (10).

Part of the difficulty in interpreting the expression for the R_L -cost in (10) is that it varies under different sets of parameters realizing the same function. In particular, the loss in (10) may vary under a trivial rescaling of the weights: for any vector $\boldsymbol{\lambda} \in \mathbb{R}^K$ with positive entries, by the 1-homogeneity of the ReLU activation we have

$$\mathbf{a}[\mathbf{W}\mathbf{x} + \mathbf{b}]_+ + c = \mathbf{a}D_{\boldsymbol{\lambda}}^{-1}[D_{\boldsymbol{\lambda}}\mathbf{W}\mathbf{x} + D_{\boldsymbol{\lambda}}\mathbf{b}]_+ + c$$

However, the value of the objective in (10) may vary between the two parameter sets $\theta = (\mathbf{W}, \mathbf{a}, \mathbf{b}, c)$ and $\theta' = (D_{\boldsymbol{\lambda}}\mathbf{W}, \mathbf{a}_{\boldsymbol{\lambda}}D_{\boldsymbol{\lambda}}^{-1}, D_{\boldsymbol{\lambda}}\mathbf{b}, c)$ realizing the same function.

To account for this scaling invariance, we define a new loss function Φ_L on pairs of inner- and outer-layer weights (\mathbf{W}, \mathbf{a}) by optimizing over all such “diagonal” rescaling of units:

$$\Phi_L(\mathbf{W}, \mathbf{a}) := \inf_{\substack{\boldsymbol{\lambda} \in \mathbb{R}^K \\ \lambda_k > 0, \forall k}} \frac{1}{L} \|\mathbf{a} \mathbf{D}_{\boldsymbol{\lambda}}^{-1}\|_2^2 + \frac{L-1}{L} \|\mathbf{D}_{\boldsymbol{\lambda}} \mathbf{W}\|_{S^q}^q \quad (11)$$

where $q := 2/(L-1)$.

Since the diagonal rescaling of units does not change the function represented by the network, we may replace the objective in (10) with $\Phi_L(\mathbf{W}, \mathbf{a})$, which gives us the following equivalent expression for the R_L -cost:

Lemma 3.3. *For any $f \in N_2(\mathbb{R}^d)$ we have*

$$R_L(f) = \min_{\theta \in \Theta_2} \Phi_L(\mathbf{W}, \mathbf{a}) \quad \text{s.t.} \quad f = h_{\theta}^{(2)}. \quad (12)$$

Previous work Neyshabur et al. (2015, 2017); Savarese et al. (2019) has shown that in the case of $L = 2$ (i.e., a single hidden-layer ReLU network with no additional linear layers), we have

$$\Phi_2(\mathbf{W}, \mathbf{a}) = \sum_{k=1}^K |a_k| \|\mathbf{w}_k\|_2. \quad (13)$$

This has been referred to as the “path norm” by Neyshabur et al. (2017). Further constraining $\|\mathbf{w}_k\|_2 = 1 \forall k$, then $\Phi_2(\mathbf{W}, \mathbf{a}) = \|\mathbf{a}\|_1$, which gives the simplified R_2 -cost in (8).

Our results suggest that no such closed-form formula exists for Φ_L with $L \geq 3$. However, the following lemma Φ_L for $L \geq 3$ gives a useful further reduction of Φ_L , which is central to the results in §4 and §5.

Lemma 3.4. *For any $\mathbf{W} \in \mathbb{R}^{K \times d}$ and $\mathbf{a} \in \mathbb{R}^K$ we have*

$$\Phi_L(\mathbf{W}, \mathbf{a}) = \inf_{\substack{\|\boldsymbol{\lambda}\|_2=1 \\ \lambda_k > 0, \forall k}} \|\mathbf{D}_{\boldsymbol{\lambda}}^{-1} \mathbf{D}_{\mathbf{a}} \mathbf{W}\|_{S^q}^{2/L} \quad (14)$$

where $q = 2/(L-1)$.

Below, we describe some further simplifications of Φ_L for special configurations of inner-layer weight matrices, and general upper and lower bounds.

The following result shows that for a certain class of \mathbf{W} matrix, $\Phi_L(\mathbf{W}, \mathbf{a})$ reduces to a group sparsity penalty on the vector of outer-layer weights, where groups correspond to clusters of co-linear rows of \mathbf{W} such that vectors associated with each cluster are mutually orthogonal.

Proposition 3.5. *Suppose each row of $\mathbf{W} \in \mathbb{R}^{K \times d}$ belongs to a set $\{\pm \mathbf{v}_1, \dots, \pm \mathbf{v}_m\}$ such that $\mathbf{v}_1, \dots, \mathbf{v}_m$ are orthonormal. For all $j = 1, \dots, m$, let \mathbf{a}_j be the vector containing the subset of outer-layer weights corresponding to rows of \mathbf{W} equal to $\pm \mathbf{v}_j$. Then we have*

$$\Phi_L(\mathbf{a}, \mathbf{W}) = \sum_{j=1}^m \|\mathbf{a}_j\|_1^{2/L}. \quad (15)$$

Two extremes of the above proposition are illustrated by the following corollaries:

Corollary 3.6. *Suppose $\mathbf{W} \in \mathbb{R}^{K \times d}$ is rank-one and has unit-norm rows and $\mathbf{a} \in \mathbb{R}^K$ is arbitrary. Then*

$$\Phi_L(\mathbf{W}, \mathbf{a}) = \|\mathbf{a}\|_1^{2/L}. \quad (16)$$

Corollary 3.7. *Suppose the rows of $\mathbf{W} \in \mathbb{R}^{K \times d}$ are orthonormal and $\mathbf{a} \in \mathbb{R}^K$ is arbitrary. Then*

$$\Phi_L(\mathbf{W}, \mathbf{a}) = \|\mathbf{a}\|_2^{2/L}. \quad (17)$$

Finally, we give some results that are particular to the $L = 3$ layer case. Note that by Lemma 3.4, the Φ_3 loss involves minimizing over the nuclear norm of a matrix, which is a convex penalty. This allows us to give the following alternative characterization of Φ_3 by way of convex duality:

Lemma 3.8. *For any $\mathbf{W} = [\mathbf{w}_1 \ \mathbf{w}_2 \ \dots \ \mathbf{w}_K]^\top \in \mathbb{R}^{K \times d}$ and $\mathbf{a} \in \mathbb{R}^K$ we have*

$$\Phi_3(\mathbf{W}, \mathbf{a}) = \max_{\|\mathbf{Q}\|_2 \leq 1} \sum_{k=1}^K |a_k \langle \mathbf{q}_k, \mathbf{w}_k \rangle|^{2/3} \quad (18)$$

where the dual variable $\mathbf{Q} = [\mathbf{q}_1 \ \mathbf{q}_2 \ \dots \ \mathbf{q}_K]^\top \in \mathbb{R}^{K \times d}$ has the same dimensions as \mathbf{W} and $\|\mathbf{Q}\|_2$ denotes the spectral norm of \mathbf{Q} (i.e., the maximum singular value of \mathbf{Q}).

The benefit of Lemma 3.8 is that it allows us to easily generate lower bounds for $\Phi_3(\mathbf{W}, \mathbf{a})$, simply by evaluating the objective in (18) at any matrix \mathbf{Q} with $\|\mathbf{Q}\|_2 \leq 1$.

Next, we give an upper-bound for Φ_3 that quantifies the interplay between low-rankness of the inner-layer weight matrix and the sparsity of the outer-layer weights:

Theorem 3.9. *Suppose $\mathbf{W} \in \mathbb{R}^{K \times d}$ is a rank- r matrix, and let $\mathbf{W} = \mathbf{U}\mathbf{\Sigma}\mathbf{V}^\top$ be a (thin) SVD, such that $\mathbf{U} \in \mathbb{R}^{K \times r}$, $\mathbf{\Sigma} = \text{diag}(\sigma_1, \dots, \sigma_r) \in \mathbb{R}^{r \times r}$, and $\mathbf{V} \in \mathbb{R}^{d \times r}$. Let $\mathbf{a} \in \mathbb{R}^K$ be arbitrary. Then*

$$\Phi_3(\mathbf{W}, \mathbf{a}) \leq \sum_{j=1}^r \left(\sigma_j \sum_{k=1}^K |a_k u_{k,j}| \right)^{2/3} \quad (19a)$$

$$= \sum_{j=1}^r \left(\sum_{k=1}^K |a_k \langle \mathbf{w}_k, \mathbf{v}_j \rangle| \right)^{2/3} \quad (19b)$$

Furthermore, equality holds when \mathbf{W} satisfies the conditions of Proposition 3.5.

Recall the definition of the “entry-wise” $\ell_{p,q}$ norm of a matrix $\mathbf{B} \in \mathbb{R}^{m \times n}$:

$$\|\mathbf{B}\|_{p,q} = \left(\sum_{j=1}^n \left(\sum_{i=1}^m |b_{i,j}|^p \right)^{q/p} \right)^{1/q};$$

a classic example is $\|\mathbf{B}\|_{2,1}$ used for group-sparse regularization in sparse coding Yuan and Lin (2006). Note that Proposition 3.5 is equivalent to

$$\Phi(\mathbf{W}, \mathbf{a}) \leq \|\mathbf{B}\|_{1, \frac{2}{3}}^{\frac{2}{3}} \text{ where } \mathbf{B} := \mathbf{D}_a \mathbf{W} \mathbf{V} = \mathbf{D}_a \mathbf{U} \mathbf{\Sigma}$$

and $\mathbf{D}_a \in \mathbb{R}^{K \times K}$ is a diagonal matrix with the entries of \mathbf{a} along the diagonal. This framing highlights that the representation cost depends not only on the alignment of the ReLU units with one another (as represented by the diagonal elements of $\mathbf{\Sigma}$ and entries of \mathbf{U}), but also the sparsity of the weights on them (i.e. the sparsity of \mathbf{a}).

4 Minimal R_L Interpolating Solutions

Minimum R_L -cost interpolants of a finite set of data can reveal important features of representation costs and their impacts. In overparameterized neural networks, there are typically many possible interpolants, and representation costs guide which of those interpolants would be selected when we fit the data using weight decay. In this section, we consider two key settings: (a) when the training features are supported on a subspace, and (b) when the training features are not supported on a subspace, but an interpolant exists which is a function of the *projection* of the features onto a subspace. The latter case is typical of overparameterized settings. All proofs of results in this section are given in Appendix B.

4.1 Training features contained in a subspace

We prove that in the special case where the training features are entirely contained in a subspace, every minimum R_L -cost interpolating solution must depend on only the projection of features onto that subspace:

Proposition 4.1. *Let $\mathcal{S} \subset \mathbb{R}^d$ denote the subspace spanned by the training features $\{\mathbf{x}_i\}_{i=1}^n$. Given any set of training labels $\{y_i\}_{i=1}^n$, let f be any minimum R_L -cost interpolating solution for any $L \geq 2$. Then*

$$f(\mathbf{x}) = f(\mathbf{P}_{\mathcal{S}}\mathbf{x})$$

for all $\mathbf{x} \in \mathbb{R}^d$, where $\mathbf{P}_{\mathcal{S}}$ is the orthogonal projector onto \mathcal{S} .

More generally, since the representation cost is translation invariant, the above result extends to the case where the training features span an affine subspace $\mathcal{A} := \{\mathbf{v} + \mathbf{x} : \mathbf{x} \in \mathcal{S}\}$ where $\mathbf{v} \in \mathcal{S}^\perp$, in which case we have $f(\mathbf{x}) = f(\mathbf{P}_{\mathcal{S}}\mathbf{x} + \mathbf{v})$.

The above proposition implies that any minimum R_L -cost interpolant f will have all its units aligned with \mathcal{S} ; i.e., every inner-layer weight vector $\mathbf{w}_k \in \mathcal{S} \forall k$. Thus, f will be constant in directions orthogonal to \mathcal{S} .

Specializing this result to the case of training features constrained to a one-dimensional subspace, we see that all minimum R_L -cost interpolants must have units aligned along the subspace (rank-one inner-layer weight matrix). Combined with Corollary 3.6, this gives the immediate corollary:

Corollary 4.2. *If the training features \mathbf{x}_i are co-linear (i.e., there exist vectors $\mathbf{u}, \mathbf{v} \in \mathbb{R}^d$ such that $\mathbf{x}_i = t_i\mathbf{u} + \mathbf{v}$ for some scalars t_i), then given any set of training labels $\{y_i\}_{i=1}^n$, the collection of minimum R_L -cost interpolating solutions is identical for all $L \geq 2$. Furthermore, every such minimizer f has aligned units, meaning it can be written in the form $f(\mathbf{x}) = \sum_{k=1}^K a_k [s_k \mathbf{u}^\top \mathbf{x} + b_k]_+ + c$, where $s_k = \pm 1$.*

The above results do not depend on the number of linear layers. However, next we show there are settings where minimum R_L -cost interpolating solutions differ for $L = 2$ and $L = 3$.

4.2 Representations supported on a subspace

Suppose that training samples may be interpolated by a function

$$f_*(\mathbf{x}) = \sum_{k=1}^K a_k [\mathbf{w}_k^\top \mathbf{x} + b_k]_+ + c, \quad (20)$$

and assume that $\|\mathbf{w}_k\| = 1 \forall k$. Given a subspace \mathcal{S} and corresponding orthogonal projection operator $\mathbf{P}_{\mathcal{S}}$ where $\mathbf{P}_{\mathcal{S}}\mathbf{w}_k \neq 0 \forall k$, we construct the function

$$g_{\mathcal{S}}(\mathbf{x}) = \sum_{k=1}^K \tilde{a}_k [\tilde{\mathbf{w}}_k^\top \mathbf{x} + \tilde{b}_k]_+ + c \quad (21)$$

where

$$\tilde{\mathbf{w}}_k := \frac{\mathbf{P}_{\mathcal{S}}\mathbf{w}_k}{\|\mathbf{P}_{\mathcal{S}}\mathbf{w}_k\|_2}, \quad \tilde{a}_k := \frac{a_k}{r_k}, \quad \tilde{b}_k := \frac{b_k a_k}{\tilde{a}_k}, \quad (22)$$

and r_k is defined as follows. Let $\mathbf{X}_k \in \mathbb{R}^{d \times n_k}$ be a matrix of the $n_k \leq n$ training samples that are “active” under ReLU unit k – that is, \mathbf{x}_i is a column of \mathbf{X}_k if $\mathbf{w}_k^\top \mathbf{x}_i + b_k > 0$. Further define $\Sigma_k := \mathbf{X}_k \mathbf{X}_k^\top$. Then we define

$$r_k := \frac{\mathbf{w}_k^\top \Sigma_k \mathbf{P}_{\mathcal{S}}\mathbf{w}_k}{\mathbf{w}_k^\top \Sigma_k \mathbf{w}_k \|\mathbf{P}_{\mathcal{S}}\mathbf{w}_k\|_2}. \quad (23)$$

If $r_k \neq 0 \forall k$, then, by construction, $g_{\mathcal{S}}$ interpolates the training samples since,

$$a_k [\mathbf{w}_k^\top \mathbf{x}_i + b_k]_+ = \tilde{a}_k [\tilde{\mathbf{w}}_k^\top \mathbf{x}_i + \tilde{b}_k]_+ \forall i, k.$$

Note that all $\tilde{\mathbf{w}}_k \in \mathcal{S}$, but, unlike the setting in Proposition 4.1, we do *not* assume that the training samples all lie in the subspace.

Given this construction, we have

$$R_2(f_*) = \sum_{k=1}^K |a_k| = \sum_{k=1}^K |\tilde{a}_k r_k| \quad (24)$$

$$R_2(g_{\mathcal{S}}) = \sum_{k=1}^K \left| \frac{a_k}{r_k} \right| = \sum_{k=1}^K |\tilde{a}_k|. \quad (25)$$

We may then conclude that

$$R_2(f_*) \leq R_2(g_{\mathcal{S}})$$

whenever

$$\left| \frac{\mathbf{w}_k^\top \sum_k \mathbf{P}_{\mathcal{S}} \mathbf{w}_k}{\mathbf{w}_k^\top \sum_k \mathbf{w}_k} \right| \leq \|P_{\mathcal{S}} \mathbf{w}_k\|_2 \quad \forall k. \quad (26)$$

In other words, the samples in \mathbf{X}_k must be more closely aligned with \mathbf{w}_k than $\mathbf{P}_{\mathcal{S}} \mathbf{w}_k$, and the ratio of these alignments must be bounded by how much of \mathbf{w}_k 's energy is in \mathcal{S} . In this case, even though $g_{\mathcal{S}}$ is an interpolating function, it may not correspond to the minimum R_2 interpolant when the feature vectors are not in the subspace \mathcal{S} (in contrast to the setting in §4.1 where, when the samples all lie in \mathcal{S} , the minimum R_2 interpolant will have all inner-layer weight vectors in \mathcal{S}).

As a special case, imagine $\mathbf{X}_k = \mathbf{w}_k \mathbf{c}_k^\top$ – that is, all training samples that activate ReLU unit k lie along the subspace spanned by \mathbf{w}_k , making $\text{rank}(\mathbf{X}_k) = 1$, and let \mathbf{w} be an orthonormal basis for a one-dimensional \mathcal{S} . (This special case is examined in detail in §5.2.) In this case, the condition in (26) is always satisfied.

To understand the three-layer representation cost, we use Lemma 3.4 and compare

$$\Phi_3(\mathbf{W}, \mathbf{a}) = \inf_{\substack{\|\boldsymbol{\lambda}\|_2=1 \\ \lambda_k > 0, \forall k}} \|D_{\boldsymbol{\lambda}}^{-1} D_{\mathbf{a}} \mathbf{W}\|_*^{2/3} \quad (27)$$

with

$$\Phi_3(\tilde{\mathbf{W}}, \tilde{\mathbf{a}}) = \inf_{\substack{\|\boldsymbol{\lambda}\|_2=1 \\ \lambda_k > 0, \forall k}} \|D_{\boldsymbol{\lambda}}^{-1} D_{\tilde{\mathbf{a}}} \tilde{\mathbf{W}}\|_*^{2/3} \quad (28)$$

corresponding to $R_3(f_*)$ and $R_3(g_{\mathcal{S}})$, respectively. Define

$$q_k := r_k \|P_{\mathcal{S}} \mathbf{w}_k\| = \frac{\mathbf{w}_k^\top \sum_k \mathbf{P}_{\mathcal{S}} \mathbf{w}_k}{\mathbf{w}_k^\top \sum_k \mathbf{w}_k} \quad (29)$$

and $\mathbf{q} := (q_1, \dots, q_K)^\top$. Then

$$\Phi_3(\tilde{\mathbf{W}}, \tilde{\mathbf{a}}) = \inf_{\substack{\|\boldsymbol{\lambda}\|_2=1 \\ \lambda_k > 0, \forall k}} \|D_{\mathbf{q}}^{-1} (D_{\boldsymbol{\lambda}}^{-1} D_{\mathbf{a}} \mathbf{W}) P_{\mathcal{S}}\|_*^{2/3}. \quad (30)$$

Differences in the R_3 representation costs associated with a two-layer ReLU network (27) and a two-layer ReLU network with an additional linear input layer (30) highlight the importance of *both* the alignment of the ReLU units (via $\mathbf{P}_{\mathcal{S}}$) and their scales (via $D_{\mathbf{q}}^{-1}$). Specifically, the $\mathbf{P}_{\mathcal{S}}$ factor ensures the product has $\text{rank} = \dim(\mathcal{S})$, and so the nuclear norm in (30) will often be smaller than that in (27). This is consistent with the intuition that an interpolating network with all ReLU units aligned with a low-dimensional subspace should have a smaller R_3 representation cost. However, despite this intuition, we show this is not always the case, and the vector \mathbf{q} , which captures the alignment of the training data with the subspace \mathcal{S} *vis-à-vis* the interpolating function f_* , can sometimes result in (27) being smaller than (30).

The expression in (30) does not admit a general analytic simplification. However, it may be computed exactly in some special cases, computed numerically, upper bounded using Theorem 3.9, and lower bounded using Lemma 3.8 with any Q . In §5, we highlight a special case in which (30) admits a simple analytical expression, allowing us to characterize the conditions under which the representation cost for the three-layer network is smaller when the ReLU units are aligned.

5 Examples illustrating ReLU alignment

5.1 Networks with ReLU weights of similar magnitudes

Suppose we have two networks that interpolate the training data with the same R_2 -cost, but one network has all its units aligned, and the other does not. Then the following result shows that the network with aligned units always has strictly lower R_3 -cost.

Proposition 5.1. *Suppose f and g are such that $R_2(f) = R_2(g)$, i.e., f and g can be described by inner-layer and outer-layer weight pairs $(\mathbf{W}_1, \mathbf{a}_2)$ and $(\mathbf{W}_2, \mathbf{a}_2)$, respectively, where both \mathbf{W}_1 and \mathbf{W}_2 have unit-norm rows, and $\|\mathbf{a}_1\|_1 = \|\mathbf{a}_2\|_1$. If \mathbf{W}_1 has rank greater than one, while \mathbf{W}_2 is rank one, then $R_3(g) < R_3(f)$.*

See Appendix C.1 for the proof.

This shows that if several networks interpolate the training data with the same R_2 -cost, yet there is one having aligned units (i.e., rank-one inner-layer weight matrix \mathbf{W}), the latter network is always the preferred fit according to the R_3 -cost.

5.2 Features on two rays

Suppose the training features $X = \{\mathbf{x}_1, \dots, \mathbf{x}_n\} \subset \mathbb{R}^d$ can be partitioned into two sets X_1, X_2 , such that $X_1 \subset R_1$ and $X_2 \subset R_2$ where R_1 and R_2 are non-colinear rays separated by half-spaces, i.e., there exist unit vectors $\mathbf{w}_1, \mathbf{w}_2 \in \mathbb{R}^2$ with $\mathbf{w}_1^\top \mathbf{w}_2 < 0$ and $\mathbf{w}_1 \neq -\mathbf{w}_2$, such that every feature $\mathbf{x}_i \in X_1$ has the form $\mathbf{x}_i = c_i \mathbf{w}_1$ for some $c_i > 0$, and every feature in $\mathbf{x}_j \in X_2$ has the form $\mathbf{x}_j = d_j \mathbf{w}_2$ for some $d_j > 0$.

Let f be any network interpolating the training data such that all units active over points in X_1 are aligned with \mathbf{w}_1 and all units active over points in X_2 are aligned with \mathbf{w}_2 :

$$f(\mathbf{x}) = \sum_{k=1}^{K_1} a_{1,k} [\mathbf{w}_1^\top \mathbf{x} + b_{1,k}]_+ + \sum_{k=1}^{K_2} a_{2,k} [\mathbf{w}_2^\top \mathbf{x} + b_{2,k}]_+.$$

Consider the related network g defined by

$$g(\mathbf{x}) = \sum_{k=1}^{K_1} \tilde{a}_{1,k} [\mathbf{w}_0^\top \mathbf{x} + \tilde{b}_{1,k}]_+ + \sum_{k=1}^{K_2} \tilde{a}_{2,k} [-\mathbf{w}_0^\top \mathbf{x} + \tilde{b}_{2,k}]_+,$$

where $\mathbf{w}_0 = \frac{\mathbf{w}_1 - \mathbf{w}_2}{\|\mathbf{w}_1 - \mathbf{w}_2\|}$ and $\tilde{a}_{j,k} := a_{j,k} / |\mathbf{w}_j^\top \mathbf{w}_0|$ and $\tilde{b}_{j,k} := |\mathbf{w}_j^\top \mathbf{w}_0| b_{j,k}$. This is the interpolating network obtained by f replacing all inner-layer weight vectors with $\pm \mathbf{w}_0$ and rescaling outer-layer weights and bias terms to satisfy interpolation constraints.

We prove that the network f whose weights aligned along the two rays always has lower R_2 -cost than associated network g with all weights aligned in one direction. However, we also prove the reverse is true of their 3-layer representation costs assuming the angle between the rays is not too large, and the size of the ℓ^1 -norms of the outer-layer weights of f are sufficiently balanced:

Proposition 5.2. *For f and g as defined above, we have $R_2(f) < R_2(g)$. Additionally, $R_3(g) < R_3(f)$ provided*

$$\frac{1}{|\cos(\theta/2)|^2} \leq 1 + 4 \frac{\|\mathbf{a}_1\|_1 \|\mathbf{a}_2\|_1}{\|\mathbf{a}\|_1^2} |\sin(\theta)|$$

where $0 < \theta \leq \pi/2$ is the smallest angle between $\mathbf{w}_1, \mathbf{w}_2$, and $\mathbf{a}_1 = (\mathbf{a}_{1,k})_{k=1}^{K_1}$, $\mathbf{a}_2 = (\mathbf{a}_{1,k})_{k=1}^{K_2}$.

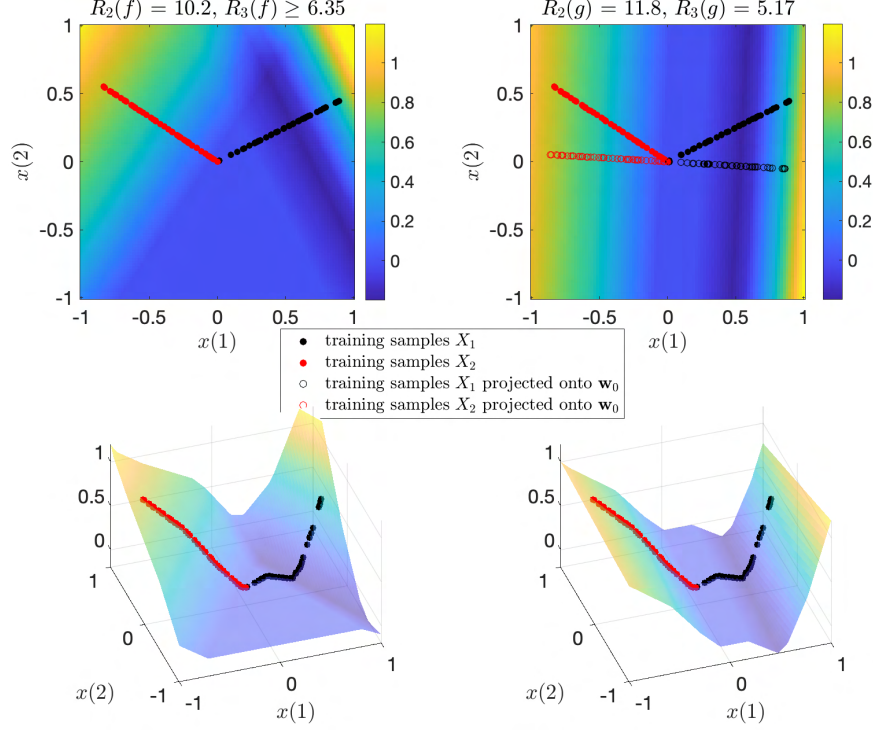


Figure 3: **Effect of learning a minimum representation cost function interpolating training samples** with either a 2-layer ReLU network or a 3-layer network with a linear layer followed by ReLU layer. *Left*: Minimum R_2 interpolant when samples lie on two rays separated by an angle of $2\pi/3$. *Right*: Minimum R_3 interpolant of same data. Both functions are perfect interpolants; see Figure 6. When the training data may be interpolated by a function of the form $f(P_S \mathbf{x})$, the linear layer promotes interpolating functions that do not vary in the direction perpendicular \mathcal{S} .

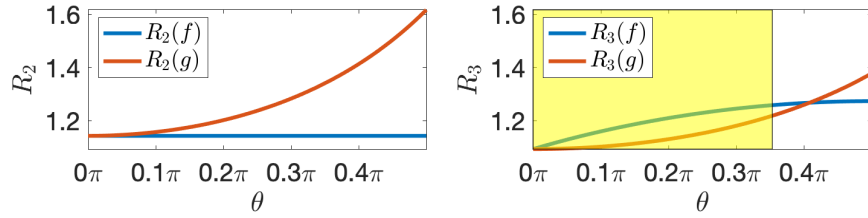


Figure 4: **An interpolant with aligned units (induced by a three-layer network with a linear layer) may have a larger R_3 representation cost than an interpolant with unaligned units, depending on the training data distribution.** Data was generated as described in §5.2 for various angles θ between the rays \mathbf{w}_1 and \mathbf{w}_2 . For most values of θ , the function g with aligned units has the lower R_3 representation cost even when it has the higher R_2 representation cost, but for some values of θ , the function f with unaligned units has lower R_3 and lower R_2 representation costs. Examples of such functions are displayed in Figure 2. The yellow region highlights the range of θ for which Proposition 5.2 predicts that the interpolant g with aligned units will have lower R_3 representation cost than the interpolant f with unaligned units.

See Appendix C.2 for the proof.

This setting with samples on two rays is illustrated in Figure 3 with $\mathbf{w}_1 = [2, 1]^\top$ and \mathbf{w}_2 is \mathbf{w}_1 rotated 120° (before normalization). Note that both f and g fit the training samples exactly but have very different behavior away from the subspaces supporting the training data. In the two-layer setting, ReLU units may be unaligned with one another, and instead align with the support of the training samples (in this case \mathbf{w}_1 and \mathbf{w}_2) in order to minimize the R_2 -cost, leading to complex behavior away from this support that presents challenges for out-of-distribution generalization analysis.

In contrast, the R_3 -cost induced by adding a linear layer promotes units that are aligned with a subspace \mathcal{S} , such that there exists some $f \in N_2(\mathbb{R}^d)$ with $y_i = f(\mathbf{P}_{\mathcal{S}}\mathbf{x}_i) \forall i$. That is, even if the training samples do not lie on a subspace, if there is a subspace onto which the samples may be projected while still admitting an interpolant, then that interpolant *may* have a lower R_3 -cost, depending on the angle θ between \mathbf{w}_1 and \mathbf{w}_2 , as shown in §5.2. The resulting alignment of the ReLU units yields less complex behavior of \hat{f} away from the support of the training samples, potentially leading to better out-of-distribution generalization.

5.3 General subspace projections

Superficially, one might think the R_3 representation cost in Lemma 3.4 associated with a network with linear layers composed with a two-layer ReLU network is lower when \mathbf{W} has lower rank – i.e. when the ReLU units are more aligned. However, the R_3 representation cost offers a more nuanced perspective because it highlights the interplay between the ReLU unit alignment with their scale (i.e. \mathbf{a}). To see this, first note that for finite training samples, we may project them all into a subspace \mathcal{S} for which no two distinct points are projected to the same location and then learn an interpolating function using these projected samples as feature vectors. As described in §4, the minimum R_L interpolant found using this procedure will have all ReLU weight vectors $\mathbf{w}_k \in \mathcal{S}$, so that $\text{rank}(\mathbf{W}) = \dim(\mathcal{S})$. In other words, it is generally possible to find interpolating functions with aligned ReLU units. However, some \mathcal{S} will lead to larger R_3 representation costs than others. As illustrated in Figure 5, a poor choice of \mathcal{S} (spanned by \mathbf{w}_0 in the figure) will lead to a configuration of projected samples that can only be interpolated by a piecewise linear function with *many* pieces (third column), while they may be interpolated with many fewer linear pieces for alternative \mathcal{S} (first column with $\mathcal{S} = \mathbb{R}^2$ and second column with $\mathcal{S} = \text{span}(\mathbf{w}_0)$). In other words, forcing ReLU units to lie in a poorly-chosen subspace may yield greater ReLU alignment by requiring many more units – i.e., by sacrificing sparsity.

The representation cost in (14) accounts for *both* the alignment (through \mathbf{W} and the nuclear norm) and the sparsity (through \mathbf{a}). From here, we may infer that adding a linear layer to a two-layer ReLU network does more than “promote alignment of ReLU units”: **when searching for interpolants of finite training datasets, training a ReLU network with additional linear layers implicitly seeks a *low-dimensional* subspace such that a *parsimonious* two-layer ReLU network can interpolate the projections of the training samples onto the subspace.** Note that we are *not* assuming that the training samples lie on a low-dimensional subspace; that is, we would not see the same effect by simply performing PCA on the training features before training the network. Rather, the best choice of subspace here depends heavily on the training labels.

6 Discussion

Past work exploring representation costs of neural networks either focused on two-layer networks Savarese et al. (2019); Ongie et al. (2019) or linear networks Dai et al. (2021). This paper is an important first step towards understanding the representation cost of *nonlinear, multi-layer* networks. The representation cost expressions we derive offer new, quantitative insights into how multi-layer networks interpolate a finite set of training samples when trained using weight decay and reflect an interaction between ReLU unit alignment and sparsity that is not captured by past representation cost analyses. Specifically, training a ReLU network with linear layers implicitly seeks a *low-dimensional* subspace such that a *parsimonious* two-layer ReLU network can interpolate the projections of the training samples onto the subspace, even when the samples themselves do not lie on a subspace. We note that ReLU alignment induced by linear layers leads to more

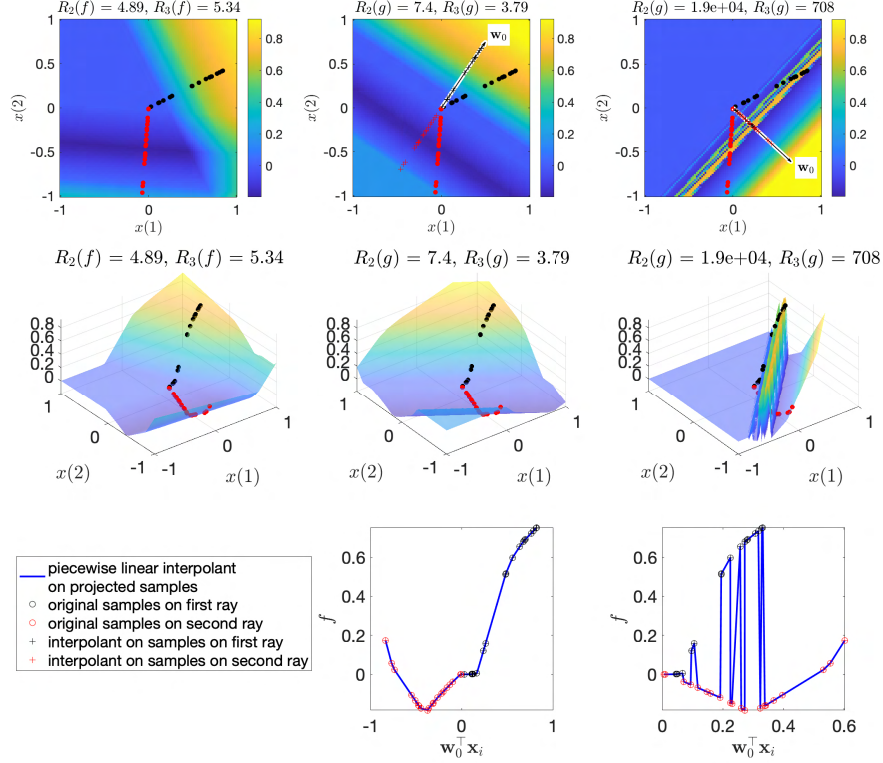


Figure 5: **Interpolating samples with aligned ReLU units** is akin to projecting samples onto a subspace (e.g., 1-D subspace w_0) and learning a piecewise linear interpolant on the subspace. Different choices of the subspace result in effective \mathbf{W} s with the same nuclear norm but vastly different representation costs R_3 . For instance, the second column shows the ideal subspace discussed in §5.2, yielding a small R_3 -cost. In contrast, the third column shows a subspace choice that requires one to learn a piecewise linear function with many more pieces, yielding a much larger R_3 -cost. These two examples have weight matrices \mathbf{W} with the same nuclear norm but different outer layer weights \mathbf{a} . Complementary plots are in Figure 7.

predictable interpolant behavior off the training data support. Specifically, §4.2 and §5.3 show that when the training data may be interpolated by a function of the form $f(\mathbf{P}_S \mathbf{x})$, using a linear layer promotes interpolating functions that do not vary in directions orthogonal to \mathcal{S} .

References

- Arora, S., Cohen, N., and Hazan, E. (2018). On the optimization of deep networks: Implicit acceleration by overparameterization. In *International Conference on Machine Learning*, pages 244–253. PMLR. <http://proceedings.mlr.press/v80/arora18a/arora18a.pdf>.
- Arora, S., Cohen, N., Hu, W., and Luo, Y. (2019). Implicit regularization in deep matrix factorization. *Advances in Neural Information Processing Systems*, 32:7413–7424.
- Ba, L. J. and Caruana, R. (2013). Do deep nets really need to be deep? *arXiv preprint arXiv:1312.6184*.
- Dai, Z., Karzand, M., and Srebro, N. (2021). Representation costs of linear neural networks: Analysis and design. *Advances in Neural Information Processing Systems*, 34.

- Daniely, A. (2017). Depth separation for neural networks. In *Conference on Learning Theory*, pages 690–696. PMLR.
- Golubeva, A., Neyshabur, B., and Gur-Ari, G. (2020). Are wider nets better given the same number of parameters? *arXiv preprint arXiv:2010.14495*. <https://arxiv.org/pdf/2010.14495.pdf>.
- Gunasekar, S., Woodworth, B., Bhojanapalli, S., Neyshabur, B., and Srebro, N. (2018). Implicit regularization in matrix factorization. In *2018 Information Theory and Applications Workshop (ITA)*, pages 1–10. IEEE.
- Hanin, B. (2019). Universal function approximation by deep neural nets with bounded width and relu activations. *Mathematics*, 7(10):992.
- Hanson, S. and Pratt, L. (1988). Comparing biases for minimal network construction with back-propagation. *Advances in neural information processing systems*, 1:177–185.
- Loshchilov, I. and Hutter, F. (2017). Decoupled weight decay regularization. *arXiv preprint arXiv:1711.05101*.
- Mulayoff, R., Michaeli, T., and Soudry, D. (2021). The implicit bias of minima stability: A view from function space. *Advances in Neural Information Processing Systems*, 34.
- Neyshabur, B., Bhojanapalli, S., Mcallester, D., and Srebro, N. (2017). Exploring generalization in deep learning. *Advances in Neural Information Processing Systems*, 30:5947–5956.
- Neyshabur, B., Tomioka, R., and Srebro, N. (2015). Norm-based capacity control in neural networks. In *Conference on Learning Theory*, pages 1376–1401. PMLR.
- Ongie, G., Willett, R., Soudry, D., and Srebro, N. (2019). A function space view of bounded norm infinite width relu nets: The multivariate case. *arXiv preprint arXiv:1910.01635*.
- Parhi, R. and Nowak, R. D. (2021). Banach space representer theorems for neural networks and ridge splines. *J. Mach. Learn. Res.*, 22(43):1–40.
- Razin, N. and Cohen, N. (2020). Implicit regularization in deep learning may not be explainable by norms. *arXiv preprint arXiv:2005.06398*.
- Razin, N., Maman, A., and Cohen, N. (2021). Implicit regularization in tensor factorization. *arXiv preprint arXiv:2102.09972*.
- Safran, I., Eldan, R., and Shamir, O. (2019). Depth separations in neural networks: what is actually being separated? In *Conference on Learning Theory*, pages 2664–2666. PMLR. <http://proceedings.mlr.press/v99/safran19a/safran19a.pdf>.
- Savarese, P., Evron, I., Soudry, D., and Srebro, N. (2019). How do infinite width bounded norm networks look in function space? In *Conference on Learning Theory*, pages 2667–2690. PMLR. <http://proceedings.mlr.press/v99/savarese19a/savarese19a.pdf>.
- Shang, F., Liu, Y., Shang, F., Liu, H., Kong, L., and Jiao, L. (2020). A unified scalable equivalent formulation for Schatten quasi-norms. *Mathematics*, 8(8):1325.
- Srebro, N., Rennie, J. D., and Jaakkola, T. S. (2004). Maximum-margin matrix factorization. In *NIPS*, volume 17, pages 1329–1336. Citeseer.
- Steinberg, D. (2005). Computation of matrix norms with applications to robust optimization. *Research thesis, Technion-Israel University of Technology*, 2.
- Urban, G., Geras, K. J., Kahou, S. E., Aslan, O., Wang, S., Caruana, R., Mohamed, A., Philipose, M., and Richardson, M. (2016). Do deep convolutional nets really need to be deep and convolutional? *arXiv preprint arXiv:1603.05691*.

- Vardi, G. and Shamir, O. (2020). Neural networks with small weights and depth-separation barriers. *arXiv preprint arXiv:2006.00625*.
- Yuan, M. and Lin, Y. (2006). Model selection and estimation in regression with grouped variables. *Journal of the Royal Statistical Society: Series B (Statistical Methodology)*, 68(1):49–67.

A Proofs of Results in Section 3

A.1 Proof of Theorem 3.1

While Theorem 3.1 can be proved by more direct means, we use the machinery developed in §3 to give a quick proof: In the univariate setting, the product of all linear-layers reduces to a column vector $\mathbf{w} \in \mathbb{R}^{K \times 1}$, which is necessarily a rank-one matrix. Therefore, Theorem 3.1 is a direct consequence of Corollary 3.6, which is a special case of Proposition 3.5, proved below.

A.2 Proof of Lemma 3.2

The result is a direct consequence of the following variational characterization of the Schatten- q quasi-norm for $q = 2/\ell$ where ℓ is a positive integer:

$$\|\mathbf{W}\|_{\mathcal{S}^{2/\ell}}^{2/\ell} = \min_{\mathbf{W}=\mathbf{W}_1\mathbf{W}_2\cdots\mathbf{W}_\ell} \frac{1}{\ell} (\|\mathbf{W}_1\|_F^2 + \|\mathbf{W}_2\|_F^2 + \cdots + \|\mathbf{W}_\ell\|_F^2)$$

where the minimization is over all matrices $\mathbf{W}_1, \dots, \mathbf{W}_\ell$ of compatible dimensions. The case $\ell = 2$ is well-known (see, e.g., Srebro et al. (2004)). The general case for $\ell \geq 3$ is established in (Shang et al., 2020, Corollary 3).

A.3 Proof of Lemma 3.4

For any fixed $\lambda > 0$, we may separately minimize over all scalar multiples $c\lambda$ where $c > 0$, to get

$$\begin{aligned} \Phi_L(\mathbf{W}, \mathbf{a}) &= \inf_{\lambda > 0} \left(\inf_{c > 0} c^2 \frac{1}{L} \|\mathbf{a} \mathbf{D}_\lambda\|_2^2 + c^{-2/(L-1)} \frac{L-1}{L} \|\mathbf{D}_\lambda^{-1} \mathbf{W}\|_{\mathcal{S}^{2/(L-1)}}^{2/(L-1)} \right) \\ &= \inf_{\lambda > 0} (\|\mathbf{a} \mathbf{D}_\lambda\|_2 \|\mathbf{D}_\lambda^{-1} \mathbf{W}\|_{\mathcal{S}^{2/(L-1)}})^{2/L} \end{aligned}$$

The last step follows by the weighted AM-GM inequality: $\frac{1}{L}a + \frac{L-1}{L}b \geq (ab^{L-1})^{1/L}$, which holds with equality when $a = b$. Here we have $a = (c\|\mathbf{a} \mathbf{D}_\lambda\|_2)^2$ and $b = (c^{-1}\|\mathbf{D}_\lambda^{-1} \mathbf{W}\|_{\mathcal{S}^{2/(L-1)}})^{2/(L-1)}$, and there exists a $c > 0$ for which $a = b$, hence we obtain the lower bound.

Finally, performing the invertible change of variables $\lambda_i = \lambda'_i/a_i$, we have $\mathbf{D}_{\lambda'}^{-1} = \mathbf{D}_\lambda^{-1} \mathbf{D}_\mathbf{a}$, and so

$$\Phi_L(\mathbf{W}, \mathbf{a}) = \inf_{\lambda' > 0} (\|\lambda'\|_2 \|\mathbf{D}_{\lambda'}^{-1} \mathbf{D}_\mathbf{a} \mathbf{W}\|_{\mathcal{S}^{2/(L-1)}})^{2/L} \quad (31)$$

$$= \inf_{\substack{\lambda' > 0 \\ \|\lambda'\|_2=1}} \|\mathbf{D}_{\lambda'}^{-1} \mathbf{D}_\mathbf{a} \mathbf{W}\|_{\mathcal{S}^{2/(L-1)}}^{2/L} \quad (32)$$

where we are able to constrain λ' to be unit norm since $\|\lambda'\|_2 \|\mathbf{D}_{\lambda'}^{-1} \mathbf{D}_\mathbf{a} \mathbf{W}\|_{\mathcal{S}^{2/(L-1)}}$ is invariant to scaling λ' by positive constants.

A.4 Proof of Proposition 3.5

We use the variational characterization of $\Phi_L(\mathbf{W}, \mathbf{a})$ given in Lemma 3.4 as an infimum over the Schatten- q quasi-norm of matrices of the form $\mathbf{D}_\lambda^{-1} \mathbf{D}_\mathbf{a} \mathbf{W}$. Fix a vector $\lambda \in \mathbb{R}^K$ with positive entries. We begin by constructing an SVD of the matrix $\mathbf{D}_\lambda^{-1} \mathbf{D}_\mathbf{a} \mathbf{W}$. Let $\mathbf{V} = [\mathbf{v}_1 \cdots \mathbf{v}_m] \in \mathbb{R}^{d \times m}$. Observe that \mathbf{W} factors as $\mathbf{W} = \mathbf{U} \mathbf{V}^\top$ where $\mathbf{U} = [\mathbf{u}_1 \cdots \mathbf{u}_m] \in \mathbb{R}^{K \times m}$ is such that $[\mathbf{u}_j]_k = \pm 1$ when the k th row of \mathbf{W} is equal to $\pm \mathbf{v}_j$ and $[\mathbf{u}_j]_k = 0$ otherwise. In particular, the vectors $\mathbf{u}_1, \dots, \mathbf{u}_m$ are mutually orthogonal, and likewise so are the vectors $\mathbf{D}_\lambda^{-1} \mathbf{D}_\mathbf{a} \mathbf{u}_1, \dots, \mathbf{D}_\lambda^{-1} \mathbf{D}_\mathbf{a} \mathbf{u}_m$. We also have $\|\mathbf{D}_\lambda^{-1} \mathbf{D}_\mathbf{a} \mathbf{u}_j\|_2 = \|\mathbf{D}_{\lambda_j}^{-1} \mathbf{a}_j\|_2 := \sigma_j$ where λ_j for all $j = 1, \dots, m$ denotes the restriction of λ to the subset of entries corresponding to rows of \mathbf{W} equal to $\pm \mathbf{v}_j$. Let $\Sigma = \mathbf{D}_\sigma$ where $\sigma = (\sigma_1, \dots, \sigma_m)$. Then $\hat{\mathbf{U}} = \mathbf{U} \Sigma^{-1}$ has orthonormal columns, and so does \mathbf{V} by assumption. This shows an SVD of $\mathbf{D}_\lambda^{-1} \mathbf{D}_\mathbf{a} \mathbf{W}$ is given by

$$\mathbf{D}_\lambda^{-1} \mathbf{D}_\mathbf{a} \mathbf{W} = \hat{\mathbf{U}} \Sigma \mathbf{V}^\top$$

In particular, σ are the singular values of $D_{\lambda}^{-1} D_a W$. Therefore, for any $q > 0$ we have

$$\|D_{\lambda}^{-1} D_a W\|_{S^q}^q = \sum_{j=1}^m \|D_{\lambda_j}^{-1} a_j\|_2^q.$$

Let $q = 2/(L-1)$. Then we have

$$\Phi_L(W, a)^{\frac{L}{L-1}} = \inf_{\substack{\lambda > 0 \\ \|\lambda\|_2=1}} \|D_{\lambda}^{-1} D_a W\|_{S^q}^q = \inf_{\substack{\lambda > 0 \\ \|\lambda\|_2=1}} \sum_{j=1}^m \|D_{\lambda_j}^{-1} a_j\|_2^q.$$

The inf on the right-hand side is equivalent to

$$\begin{aligned} \inf_{\substack{c_j > 0 \\ \sum_{j=1}^m c_j^2=1}} \inf_{\substack{\lambda_j > 0 \\ \|\lambda_j\|_2=c_j}} \sum_{j=1}^m \|D_{\lambda_j}^{-1} a_j\|_2^q &= \inf_{\substack{c_j > 0 \\ \sum_{j=1}^m c_j^2=1}} \sum_{j=1}^m \inf_{\substack{\lambda_j > 0 \\ \|\lambda_j\|_2=c_j}} \|D_{\lambda_j}^{-1} a_j\|_2^q \\ &= \inf_{\substack{c_j > 0 \\ \sum_{j=1}^m c_j^2=1}} \sum_{j=1}^m \left(\frac{1}{c_j} \|a_j\|_1 \right)^q \\ &= \left(\sum_{j=1}^m \|a_j\|_1^{2/L} \right)^{\frac{L}{L-1}} \end{aligned}$$

where the final equality follows from an application of Lemma 3.1 in Steinberg (2005), proving the claim.

A.5 Proof of Lemma 3.8

Starting from Lemma 3.4, we have

$$\Phi_3(W, a) = \inf_{\substack{\lambda > 0 \\ \|\lambda\|_2=1}} \|D_{\lambda}^{-1} D_a W\|_*^{2/3}.$$

Since the operator norm is the convex dual of the nuclear norm, the right-hand-side above is equivalent to

$$\inf_{\substack{\lambda > 0 \\ \|\lambda\|_2=1}} \max_{\|Q\| \leq 1} \langle D_{\lambda}^{-1} D_a W, Q \rangle^{2/3}$$

where the maximum is over all Q having the same dimensions as Q and $\|Q\|$ denotes the spectral norm of Q , and $\langle W, Q \rangle = \text{Tr } W^{\top} Q$. Equivalently, expanding the trace inner product in terms of the rows of W and Q we have

$$\Phi_3(W, a) = \inf_{\substack{\lambda > 0 \\ \|\lambda\|_2=1}} \max_{\|Q\| \leq 1} \left(\sum_{k=1}^K \frac{a_k \langle w_k, q_k \rangle}{\lambda_k} \right)^{2/3}$$

where w_i and q_i denote the i th row of W and Q , respectively. By Sion's minimax theorem, we may exchange the order of the inf and max, to get

$$\Phi_3(W, a) = \max_{\|Q\| \leq 1} \inf_{\substack{\lambda > 0 \\ \|\lambda\|_2=1}} \left(\sum_{k=1}^K \frac{a_k \langle w_k, q_k \rangle}{\lambda_k} \right)^{2/3} = \max_{\|Q\| \leq 1} \sum_{k=1}^K |a_k \langle w_k, q_k \rangle|^{2/3}$$

where the final equality follows from an application of Lemma 3.1 in Steinberg (2005).

B Proofs of Results in Section 4

B.1 Proof of Proposition 4.1

This result is most easily shown using the initial formulation of the data interpolating problem (5) as minimizing the Euclidean norm of the weights $C_L(\theta)$ in an L -layer representation.

Let $f = h_\theta^{(L)}$ be any minimum $C_L(\theta)$ interpolant of the training data, whose first layer weight matrix is \mathbf{W}_1 . Let \mathcal{S} be the subspace spanned by the training data locations, and let $\mathbf{P}_\mathcal{S}$ be the orthogonal projector onto \mathcal{S} . We will show that $\mathbf{W}_1 = \mathbf{W}_1 \mathbf{P}_\mathcal{S}$, and so $f(\mathbf{x}) = f(\mathbf{P}_\mathcal{S} \mathbf{x})$.

Suppose, by way of contradiction, that $\mathbf{W}_1 \neq \mathbf{W}_1 \mathbf{P}_\mathcal{S}$, or equivalently, $\mathbf{W}_1(\mathbf{I} - \mathbf{P}_\mathcal{S}) \neq \mathbf{0}$. By the Pythagorean theorem we have

$$\|\mathbf{W}_1\|_F^2 = \|\mathbf{W}_1 \mathbf{P}_\mathcal{S}\|_F^2 + \|\mathbf{W}_1(\mathbf{I} - \mathbf{P}_\mathcal{S})\|_F^2$$

which implies

$$\|\mathbf{W}_1\|_F^2 > \|\mathbf{W}_1 \mathbf{P}_\mathcal{S}\|_F^2$$

where the inequality is strict since by the assumption $\mathbf{W}_1(\mathbf{I} - \mathbf{P}_\mathcal{S}) \neq \mathbf{0}$. Also, since $\mathbf{x}_i \in \mathcal{S}$ for all $i = 1, \dots, n$, we have $\mathbf{W}_1 \mathbf{x}_i = \mathbf{W}_1 \mathbf{P}_\mathcal{S} \mathbf{x}_i$. Therefore, the cost $C_L(\theta)$ is always strictly reduced by replacing \mathbf{W}_1 with $\widetilde{\mathbf{W}}_1 = \mathbf{W}_1 \mathbf{P}_\mathcal{S}$, while the data fit is left unchanged, violating the assumption that \mathbf{W}_1 belonged to a minimizing set of parameters, which proves the claim.

B.2 Proof of Corollary 4.2

Without loss of generality, we may translate the data points so that they lie on a one-dimensional linear subspace.

Let $f(\mathbf{x}) = \mathbf{a}^\top [\mathbf{W} \mathbf{x} + \mathbf{b}]_+ + c$ be any minimum R_L -norm interpolant. Because we can rescale the rows of \mathbf{W} and the corresponding entries of \mathbf{a} without changing the representation cost, we may assume \mathbf{W} has unit-norm rows. Also, since the data is co-linear, Proposition 4.1 shows that

$$f(\mathbf{x}) = f(\mathbf{P}_\mathcal{S} \mathbf{x})$$

where \mathcal{S} is the one-dimensional subspace spanned by the data locations. This implies that the inner-layer weight matrix \mathbf{W} is rank one of the form $\mathbf{W} = \mathbf{s} \mathbf{u}^\top$. Therefore, by Corollary 3.6, we have

$$\Phi_L(\mathbf{W}, \mathbf{a}) = \|\mathbf{a}\|_1^{2/L}$$

Since $\|\mathbf{a}\|_1^{2/L}$ is a monotonic transformation of $\|\mathbf{a}\|_1$, the sets of minimizing R_L -interpolating solutions for all $L \geq 2$ must coincide, similar to the univariate case.

C Proofs of Results in Section 5

C.1 Proof of Proposition 5.1

We first prove two lemmas:

Lemma C.1. *For any vector $\mathbf{a} \in \mathbb{R}^K$ we have*

$$\inf_{\substack{\lambda > 0 \\ \|\lambda\|_2 = 1}} \|D_\lambda^{-1} \mathbf{a}\|_2^2 = \|\mathbf{a}\|_1^2$$

Proof. This can be shown directly by optimizing the Lagrangian corresponding to the squared objective:

$$\mathcal{L}(\lambda, \sigma) = \sum_k \frac{|a_k|^2}{\lambda_k^2} + \sigma \left(1 - \sum_k \lambda_k^2 \right)$$

Straightforward calculations show that the only critical point of the Lagrangian is where $\lambda_k = |a_k|^{1/2} / \|\mathbf{a}\|_1^{1/2}$, which gives the claim. \square

Lemma C.2.

$$\inf_{\substack{\boldsymbol{\lambda} \in \mathbb{R}^K \\ \lambda_k > 0 \\ \|\boldsymbol{\lambda}\|_2 = 1}} \prod_{k=1}^K \frac{1}{\lambda_k^2} = K^K.$$

Proof. We show the inf is attained where $\lambda_1 = \dots = \lambda_K = 1/\sqrt{K}$. Suppose it is not, so that there exists indices $i \neq j$ such that $\lambda_i \neq \lambda_j$. Holding all the other λ_k fixed, consider all $\alpha, \beta > 0$ subject to the constraints $\alpha^2 + \beta^2 = C$ where $C = 1 - \sum_{k \neq i, j} \lambda_k^2$ is constant. Then the optimizer of

$$\inf_{\substack{\alpha, \beta > 0 \\ \alpha^2 + \beta^2 = C}} \frac{1}{\alpha\beta}$$

occurs where $\alpha = \beta$, hence by replacing λ_i with λ_j with their common value, we would be able to reduce the original objective, violating the assumption that λ_i and λ_j were minimizers. Therefore, $\lambda_i = \lambda_j$ for all i, j , which implies $\lambda_k = 1/\sqrt{K}$ for all k . \square

Now we prove Proposition 5.1. Let $\mathbf{a} \in \mathbb{R}^K$ and suppose $\mathbf{W} \in \mathbb{R}^{K \times d}$ is such that $r := \text{rank}(\mathbf{W}) > 1$. Fix a unit-norm weighting vector $\boldsymbol{\lambda}$ with positive entries. Let $\sigma_1, \dots, \sigma_r$ be the singular values of the matrix $\mathbf{D}_{\boldsymbol{\lambda}}^{-1} \mathbf{D}_{\mathbf{a}} \mathbf{W}$. Then we have

$$\|\mathbf{D}_{\boldsymbol{\lambda}}^{-1} \mathbf{D}_{\mathbf{a}} \mathbf{W}\|_*^2 = \left(\sum_{i=1}^r \sigma_i \right)^2 = \sum_{i=1}^r \sigma_i^2 + 2 \sum_{i>j} \sigma_i \sigma_j$$

Note that

$$\left(\sum_{i=1}^r \sigma_i \right)^2 = \|\mathbf{D}_{\boldsymbol{\lambda}}^{-1} \mathbf{D}_{\mathbf{a}} \mathbf{W}\|_F^2 = \|\mathbf{D}_{\boldsymbol{\lambda}}^{-1} \mathbf{a}\|_2^2$$

and by Lemma C.1 we have

$$\inf_{\substack{\boldsymbol{\lambda} > 0 \\ \|\boldsymbol{\lambda}\|_2 = 1}} \sum_{i>j} \|\mathbf{D}_{\boldsymbol{\lambda}}^{-1} \mathbf{a}\|_2^2 = \|\mathbf{a}\|_1^2$$

Also, since there are $r(r-1)/2$ terms in the sum $\sum_{i>j} \sigma_i \sigma_j$, and each σ_i appears as a factor $r-1$ times, by the AM-GM inequality we have

$$\sum_{i>j} \sigma_i \sigma_j \geq \frac{2}{r(r-1)} \left(\prod_{i=1}^r \sigma_i^2 \right)^{\frac{1}{r}}$$

Since $\mathbf{Q} := \mathbf{D}_{\boldsymbol{\lambda}} \mathbf{D}_{\mathbf{a}} \mathbf{W}$ is rank r there exists a subset of r rows of \mathbf{Q} such that its restriction to these rows is also rank r . Collect the indices of these rows into a set Ω , and let $\mathbf{P}_{\Omega} \in \mathbb{R}^{r \times K}$ be the matrix that restricts onto indices in Ω . If we let $\tilde{\sigma}_i$ denote the i th singular value of $\mathbf{P}_{\Omega} \mathbf{Q}$, observe that $0 < \tilde{\sigma}_i \leq \sigma_i$ for all $i = 1, \dots, r$. Therefore,

$$\prod_{i=1}^r \sigma_i^2 \geq \prod_{i=1}^r \tilde{\sigma}_i^2 = \det(\mathbf{P}_{\Omega} \mathbf{Q} \mathbf{Q}^{\top} \mathbf{P}_{\Omega}^{\top}) = \frac{\prod_{k \in \Omega} |a_k|^2}{\prod_{k \in \Omega} \lambda_k^2} \det(\mathbf{P}_{\Omega} \mathbf{W} \mathbf{W}^{\top} \mathbf{P}_{\Omega}^{\top})$$

Also, by Lemma C.2

$$\inf_{\substack{\boldsymbol{\lambda} > 0 \\ \|\boldsymbol{\lambda}\|_2 = 1}} \frac{1}{\prod_{k \in \Omega} \lambda_k^2} = r^r$$

since we can shrink all λ_k with $k \notin \Omega$ to zero. Therefore, setting $C = (\prod_{k \in \Omega} |a_k|^2) \det(\mathbf{P}_{\Omega} \mathbf{W} \mathbf{W}^{\top} \mathbf{P}_{\Omega}^{\top}) > 0$, we have shown

$$\inf_{\substack{\boldsymbol{\lambda} > 0 \\ \|\boldsymbol{\lambda}\|_2 = 1}} 2 \sum_{i>j} \sigma_i \sigma_j \geq \frac{4C^{1/r}}{r-1}$$

Finally, putting the above pieces together, we have

$$\Phi_3(\mathbf{W}, \mathbf{a})^3 = \inf_{\substack{\lambda > 0 \\ \|\lambda\|_2 = 1}} \|D_\lambda^{-1} D_a \mathbf{W}\|_*^2 = \inf_{\substack{\lambda > 0 \\ \|\lambda\|_2 = 1}} \sum_{i=1}^r \sigma_i^2 + 2 \sum_{i>j} \sigma_i \sigma_j \quad (33)$$

$$\geq \inf_{\substack{\lambda > 0 \\ \|\lambda\|_2 = 1}} \sum_{i=1}^r \sigma_i^2 + \inf_{\substack{\lambda > 0 \\ \|\lambda\|_2 = 1}} 2 \sum_{i>j} \sigma_i \sigma_j \quad (34)$$

$$\geq \|\mathbf{a}\|_1^2 + \frac{4C^{1/r}}{r-1} \quad (35)$$

and since $\frac{4C^{1/r}}{r-1} > 0$ we see that $\Phi_3(\mathbf{W}, \mathbf{a}) > \|\mathbf{a}\|_1^{2/3}$, as claimed.

C.2 Proof of Proposition 5.2

First, since g has rank-one weights, we can compute $\Phi_3(g)$ exactly using Corollary 3.6:

$$\Phi_3(g) = \left(|\langle \mathbf{w}_0, \mathbf{w}_1 \rangle|^{-1} \sum_{k=1}^{K_1} \|\mathbf{a}_1\|_1 + |\langle \mathbf{w}_0, \mathbf{w}_2 \rangle|^{-1} \|\mathbf{a}_2\|_1 \right)^{2/3} = \left(\frac{\|\mathbf{a}\|_1}{\cos(\theta/2)} \right)^{2/3}$$

Next we lower bound Φ_3 using the equivalence

$$\Phi_3(f) = \inf_{\substack{\lambda > 0 \\ \|\lambda\| = 1}} \|D_\lambda^{-1} D_a \mathbf{W}\|_*^{2/3}.$$

Fix any $\lambda > 0$. We begin by computing an SVD of $\mathbf{M} = D_\lambda^{-1} D_a \mathbf{W}$. Observe that $\mathbf{W} = \mathbf{U} \begin{bmatrix} \mathbf{w}_1^\top \\ \mathbf{w}_2^\top \end{bmatrix}$ where $\mathbf{U} = [\mathbf{u}_1 \mathbf{u}_2]$ with $(\mathbf{u}_1)_k = 1$ when the k th row of \mathbf{W} is \mathbf{w}_1 and 0 otherwise, and vice-versa for \mathbf{u}_2 . In particular, \mathbf{u}_1 and \mathbf{u}_2 are orthogonal, and so are $D_\lambda^{-1} D_a \mathbf{u}_1$ and $D_\lambda^{-1} D_a \mathbf{u}_2$. Note that the norms of these vectors are $\|D_{\lambda_1}^{-1} \mathbf{a}_1\|$ and $\|D_{\lambda_2}^{-1} \mathbf{a}_2\|$, where D_{λ_1} and D_{λ_2} denote restrictions of λ to indices corresponding to the weights in \mathbf{a}_1 and \mathbf{a}_2 , respectively.

Let $\hat{\mathbf{U}} \hat{\Sigma} \hat{\mathbf{V}}^\top$ be an SVD of the 2×2 matrix

$$\mathbf{Q} := \begin{bmatrix} \|D_{\lambda_1}^{-1} \mathbf{a}_1\|_2 \mathbf{w}_1^\top \\ \|D_{\lambda_2}^{-1} \mathbf{a}_2\|_2 \mathbf{w}_2^\top \end{bmatrix} = \begin{bmatrix} \|D_{\lambda_1}^{-1} \mathbf{a}_1\|_2 & 0 \\ 0 & \|D_{\lambda_2}^{-1} \mathbf{a}_2\|_2 \end{bmatrix} \begin{bmatrix} \mathbf{w}_1^\top \\ \mathbf{w}_2^\top \end{bmatrix}$$

Then an SVD of $D_a \mathbf{W}$ is

$$D_a \mathbf{W} = \left(D_a \mathbf{U} \begin{bmatrix} \|D_{\lambda_1}^{-1} \mathbf{a}_1\|_2^{-1} & 0 \\ 0 & \|D_{\lambda_2}^{-1} \mathbf{a}_2\|_2^{-1} \end{bmatrix} \hat{\mathbf{U}} \right) \hat{\Sigma} \hat{\mathbf{V}}^\top$$

This shows that the singular values of \mathbf{M} coincide with those of the matrix \mathbf{Q} . Let σ_1 and σ_2 be their two non-zero singular values. Then, we have the identities:

$$(\sigma_1 + \sigma_2)^2 = \sigma_1^2 + \sigma_2^2 + 2\sigma_1\sigma_2 \quad (36)$$

$$= \|\mathbf{Q}\|_F^2 + 2 \det(\mathbf{Q} \mathbf{Q}^\top)^{1/2} \quad (37)$$

$$= \|D_\lambda^{-1} \mathbf{a}\|_2^2 + 2 \|D_{\lambda_1}^{-1} \mathbf{a}_1\|_2 \|D_{\lambda_2}^{-1} \mathbf{a}_2\|_2 |\sin(\theta)| \quad (38)$$

Next we optimize the last two terms *separately* over λ to get a lower bound. These can be optimized exactly using simple Lagrange multiplier arguments, to give:

$$\inf_{\substack{\lambda > 0 \\ \|\lambda\|_2 = 1}} \|D_\lambda^{-1} \mathbf{a}\|_2^2 = \|\mathbf{a}\|_1^2$$

and

$$\inf_{\substack{\lambda_1, \lambda_2 > 0 \\ \|\lambda_1\|_2^2 + \|\lambda_2\|_2^2 = 1}} \|D_{\lambda_1}^{-1} \mathbf{a}_1\|_2 \|D_{\lambda_2}^{-1} \mathbf{a}_2\|_2 = 2\|\mathbf{a}_1\|_1 \|\mathbf{a}_2\|_1$$

Therefore, we have shown

$$\Phi_3(f) \geq (\|\mathbf{a}\|_1^2 + 4\|\mathbf{a}_1\|_1 \|\mathbf{a}_2\|_1 |\sin(\theta)|)^{1/3} \quad (39)$$

$$= \|\mathbf{a}\|_1^{2/3} \left(1 + 4 \frac{\|\mathbf{a}_1\|_1 \|\mathbf{a}_2\|_1}{\|\mathbf{a}\|_1^2} |\sin(\theta)| \right)^{1/3} \quad (40)$$

Finally, comparing this to the expression for $\Phi_3(g)$ and cancelling the factor of $\|\mathbf{a}\|_1^{2/3}$ gives the claim.

D Supplemental figures

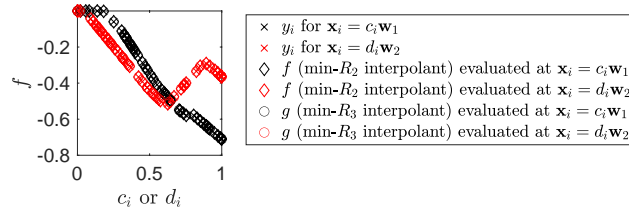


Figure 6: Empirical confirmation that both functions f and g in Figure 3 are perfectly interpolating the training data.

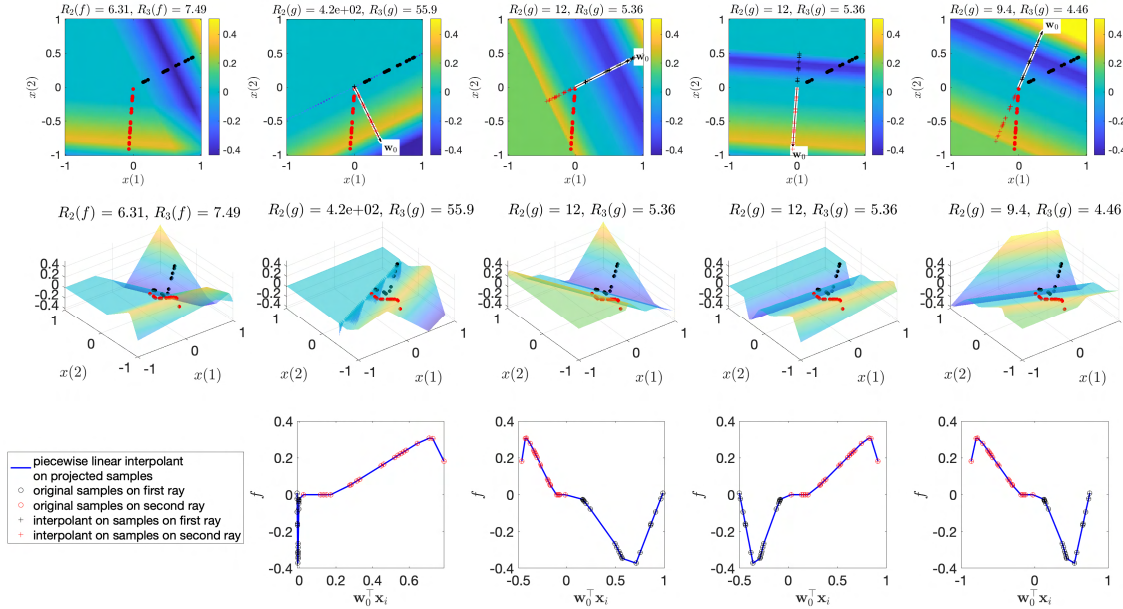


Figure 7: Interpolating samples with aligned ReLU units like Figure 5 with different subspaces \mathbf{w}_0 .